IEICE TRANSACTIONS

on Fundamentals of Electronics, Communications and Computer Sciences

VOL. E99-A NO. 7
JULY 2016

A PUBLICATION OF THE ENGINEERING SCIENCES SOCIETY
The Institute of Electronics, Information and Communication Engineers
Kikai-Shinko-Kaikan Bldg., 5-8, Shibakoen 3 chome, Minato-ku, TOKYO, 105-0011 JAPAN

PAPER

Performance of APD-Based Amplify-and-Forward Relaying FSO Systems over Atmospheric Turbulence Channels*

Thanh V. PHAM[†], *Nonmember and* **Anh T. PHAM**[†a)], *Member*

SUMMARY This paper proposes and theoretically analyzes the performance of amplify-and-forward (AF) relaying free-space optical (FSO) systems using avalanche photodiode (APD) over atmospheric turbulence channels. APD is used at each relay node and at the destination for optical signal conversion and amplification. Both serial and parallel relaying configurations are considered and the subcarrier binary phase-shift keying (SC-BPSK) signaling is employed. Closed-form expressions for the outage probability and the bit-error rate (BER) of the proposed system are analytically derived, taking into account the accumulating amplification noise as well as the receiver noise at the relay nodes and at the destination. Monte-Carlo simulations are used to validate the theoretical analysis, and an excellent agreement between the analytical and simulation results is confirmed.

key words: *relaying free-space optics, amplify-and-forward, atmospheric turbulence, APD receiver, outage probability, bit-error rate, log-normal distribution*

1. Introduction

The rapidly increasing demand for high data-rate wireless transmission has led to the recent development of free-space optical (FSO) communications. Operating at unlicensed optical frequencies, FSO also effectively addresses the spectrum scarcity problem in wireless radio-frequency (RF) communications [1], [2]. It has been previously shown that the performance of FSO systems is negatively affected by various atmospheric conditions. On one hand, it is the effect of signal scattering (caused by dust particles, water droplets from fog, rain or snow) and absorption (primarily due to water vapour and carbon dioxide). These impairments considerably limit the visibility of practical FSO systems. On the other hand, even with good visibility, atmospheric turbulence, which results in intensity fluctuation of the optical signal and eventually degrades the system performance, remains a challenging issue. Previous studies revealed that the transmission channel of FSO systems, under the impact of atmospheric turbulence, is limited to two km regardless of the degree of visibility [3]. Thus, methods for mitigating the impact of turbulence-induced fading are of particular interest in FSO communications.

As turbulence strength is proportional to the link distance, the use of relay nodes is an effective method to improve the link availability as well as the performance of FSO systems [4]–[9]. Relaying FSO systems are also more applicable in practice because there are usually obstacles along the transmission path and thus the light-of-sight (LOS) condition is not always available. Similar to their RF counterparts, relaying FSO systems can be implemented in either decode-and-forward (DF) or amplify-and-forward (AF) strategy, of which the latter requires less computing power as no decoding or quantizing operation is performed at relay nodes.

Many studies on the performance of AF relaying FSO systems, including both conventional electrical AF [7], [10], [11] and all-optical AF using optical amplifiers, such as erbium-doped fiber amplifiers (EDFA) [12]–[14], have appeared in the literature. In this study, we propose a novel structure of AF relay node by using avalanche photodiode (APD) as an amplification device. Due to the internal amplification feature of the APD, the proposed relay node is simpler than that of an electrical AF relaying where a separate electrical amplifier is required. Furthermore, the use of APD, with a much larger receiving area, also relaxes the requirement of the complex beam tracking and control in EDFA-based AF systems for guiding received optical beam into the fiber of EDFA. As a matter of fact, APD was also proposed for DF relaying in our previous study, and we named it amplify-decoded-forward (ADF) system [6]. The ADF is actually a special type of the DF, and it therefore also requires a similar computing power as the conventional DF does.

For the newly proposed APD-based AF system, we analytically derive closed-form expressions for the outage probability and the bit-error rate (BER), taking into account both signal-dependent noises (including APD amplification noise and receiver noise) and the impact of atmospheric turbulence. It is important to note that the performance of AF relaying FSO systems considering amplification noise over turbulence channels has been recently reported [15]–[17]. Nevertheless, due to the analysis complexity, these studies were limited to the case of single-relay dual-hop AF (i.e., there is only one relay node between the source and the destination). In our study, the generalized case of AF relaying systems with an arbitrary number of nodes will be presented. Relay nodes can be arranged in either serial or parallel fashion corresponding to serial or parallel configurations (also known as parallel dual-hop relaying), respectively. In addition, we characterize the turbulence channel by a log-normal distribution [7], [9], [12], [18], [19], which is commonly used to model weak-to-moderate turbulence conditions. The subcarrier binary phase-shift keying (SC-BPSK) modulation

Manuscript received December 16, 2015.
Manuscript revised March 4, 2016.

[†]The authors are with the Computer Communications Lab., The University of Aizu, Aizuwakamatsu-shi, 965-8580 Japan.

*The paper has been presented in part at IEEE GLOBECOM OWC 2013.

a) E-mail: pham@u-aizu.ac.jp

DOI: 10.1587/transfun.E99.A.1455

is employed with the deployment of an APD receiver at the destination node. It has been previously confirmed that, in the presence of atmospheric turbulence, BPSK outperforms the popular on-off keying (OOK) scheme thanks to the use of fixed "zero" decision threshold [20]. Finally, to validate the analytical method, Monte Carlo simulations are performed, and an excellent agreement between simulation and theoretical results is observed.

The remainder of the paper is organized as follows. In Sect. 2, we describe the proposed APD-based AF relaying FSO system model, channel model and related noises for serial and parallel configurations. The theoretical performance analysis, including the derivations of closed-form expressions of the system outage probability and BER, is presented in Sect. 3. Section 4 presents some representative numerical results and discussions. Finally, we conclude the paper in Sect. 5.

2. System Descriptions

We consider APD-based AF relaying FSO systems, in which a signal from the source to the destination is propagated through N relay nodes. Figure 1 shows the model of an APD-based AF relay node. The received electrical signal obtained from the APD will be used to modulate the intensity of the optical beam, and then relayed to the following node. Here, the APD is used for both optical-to-electrical conversion and amplification of the converted electrical current. The receiver noise at each relay node is also amplified and forwarded to the next transmission. Figure 2 describes a serial relaying configuration where a signal from the source is consecutively transmitted to the destination through N relay nodes. In a parallel relaying configuration, as shown in Fig. 3, the source is equipped with a multi-laser transmitter with each of the lasers pointing out to a corresponding relay node. At each relay node, the incoming signal is also converted, amplified, and then modulated for being relayed to the destination. In both serial and parallel configurations, an APD receiver is used at the destination node. The received signal at the destination is therefore amplified before being electrically demodulated by a BPSK demodulator, then finally decoded to recover the original data.

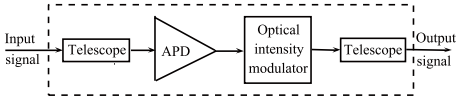

Fig. 1 APD-based AF relay node model.

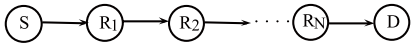

Fig. 2 Serial relaying configuration.

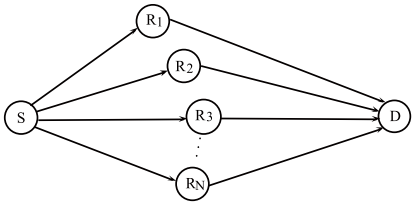

Fig. 3 Parallel relaying configuration.

2.1 Channel Model

In weak-to-moderate turbulence conditions, it is generally accepted that the turbulence-induced fading can be modeled as a random process X with log-normal distribution [18]. Assuming that the average fading amplitude is normalized to unity, the probability density function (pdf) of X is then given by

$$f_X(x) = \frac{1}{\sqrt{2\pi}\sigma_s(\ell)x} \exp\left[-\frac{\left(\ln x + \sigma_s^2(\ell)\right)^2}{2\sigma_s^2(\ell)}\right]. \quad (1)$$

The log intensity variance $\sigma_s^2(\ell)$ strongly depends on the channel characteristics and the distance between two terminals as

$$\sigma_s^2(\ell) = \exp\left[\frac{0.49\sigma_R^2(\ell)}{\left(1 + 0.18d^2 + 0.56\sigma_R^{\frac{12}{5}}(\ell)\right)^{\frac{7}{6}}} + \frac{0.51\sigma_R^2(\ell)}{\left(1 + 0.9d^2 + 0.62d^2\sigma_R^{\frac{12}{5}}(\ell)\right)^{\frac{5}{6}}}\right] - 1, \quad (2)$$

in which, $d = \sqrt{kD^2/4\ell}$, with ℓ is the distance between two terminals and D is the receiver aperture diameter. $k = 2\pi/\lambda$, where λ denotes the optical wavelength, is the optical wave number [3]. $\sigma_R^2(\ell)$ is the distance-dependent Rytov variance, and in case of plane wave propagation, it is derived by

$$\sigma_R^2(\ell) = 1.23C_n^2k^{7/6}\ell^{11/6}, \quad (3)$$

where C_n^2 is the altitude-dependent index of the refractive structure parameter, which determines the turbulence strength. Typically, C_n^2 varies from 10^{-17} m$^{-2/3}$ for weak turbulence to 10^{-13} m$^{-2/3}$ for strong turbulence [21].

2.2 APD Shot Noise and Thermal Noise

Now, we consider the APD shot noise and thermal noise at relay nodes when the SC-BPSK signaling is employed. In the AF model, the received optical signal is converted to an electrical current and then amplified by an APD. The obtained electrical signal is not decoded but used to re-modulate the intensity of the laser source to generate an optical beam for the next transmission. We first derive the received signal and the receiver noise for single hop FSO systems using APD with SC-BPSK modulation, and set it as a benchmark for later uses in different configurations. First, the transmitted

optical signal can be expressed as

$$s(t) = \frac{P_s}{2}\left[1 + \cos(2\pi f_c t + b_k\pi)\right]. \quad (4)$$

Here, P_s is the peak transmitted optical power in the case of no turbulence, f_c is the subcarrier frequency and $b_k \in \{0, 1\}$ denotes the binary data signal. The received optical signal due to the impact of both distance-dependent channel loss and turbulence-induced fading is written as

$$P(t) = aX\frac{P_s}{2}\left[1 + \cos(2\pi f_c t + b_k\pi)\right], \quad (5)$$

where a, X are the channel loss and the scintillation caused by atmospheric turbulence, respectively. The channel loss is the result of molecular absorption and aerosol scattering suspended in the air and given by [2]

$$a = \frac{A_r}{\pi(\frac{\phi\ell}{2})^2}\exp(-\beta_\nu \ell), \quad (6)$$

where $A_r, \phi, \ell, \beta_\nu$ represent the area of receiver aperture, the optical beam divergence angle in radian, the link length of the FSO link and the atmospheric extinction coefficient, respectively.

Since the scintillation X varies slowly enough, the DC term $\{aXP_s/2\}$ can be filtered out by a bandpass filter. Hence, the output electrical signal of the APD can be written as

$$r(t) = \Re\bar{g}\frac{P_s}{2}aX\cos(2\pi f_c t + b_k\pi) + n(t), \quad (7)$$

where $\Re, \bar{g}$, and $n(t)$ denote the responsivity, the average APD gain and the receiver noise, respectively. The receiver noise term $n(t)$ includes thermal noise and shot noise and can be well modeled as a stationary Gaussian random process whose variance is given by

$$\sigma^2 = \frac{4k_B T}{R_L}F_n\Delta f + 2q\bar{g}^2F_A\Re\left(\frac{P_s}{4}aX\right)\Delta f, \quad (8)$$

where $k_B, T, R_L, F_n, q, \Delta f, F_A$ represent the Boltzmann constant, the absolute temperature of the receiver, the APD's load resistance, the amplifier noise figure, the electron charge, the effective noise bandwidth, and the exceed noise factor, respectively [3]. Typically, $\Delta f = R_b/2$ is selected, where R_b is the system bit rate; $F_A = k_A\bar{g} + (1 - k_A)(2 - \frac{1}{\bar{g}})$, where k_A is the ionization factor.

2.3 APD-Based AF Relaying FSO System

In this part, we use the indexes $\{0, 1, .., N, N + 1\}$ for indicating the source, the N relay nodes and the destination, respectively. We also assume that the parameters of all APD receivers at relay nodes are the same, and the atmospheric turbulence at all hops are independent and identically distributed. Furthermore, the notation $\chi_{i,j}$ is used to indicate a certain quantity χ (e.g., path loss, atmospheric turbulence) of the hop connecting the $i-$th and the $j-$th nodes.

For the sake of simplicity, in both relaying configurations, we also assume that the optical power P_s allocating at the source and all relay nodes are the same and thus given by

$$P_s = \frac{P_t}{N_r} = \begin{cases} \frac{P_t}{N+1} & \text{for serial configuration,} \\ \frac{P_t}{2N} & \text{for parallel configuration,} \end{cases} \quad (9)$$

where P_t is the total transmitted power of the whole system. N_r is the number of relay hops, which equals to $N + 1$ in the case of serial configuration or $2N$ in the case of parallel one. Based on the benchmark developed in Sect. 2.2, we now investigate the performance of two relaying configurations as follows.

2.3.1 Serial Configuration

In serial relaying, the output electrical signal of the APD at the first relay node is written following Eq. (7) as

$$r_1(t) = \Re\bar{g}\frac{P_s}{2}a_{0,1}X_{0,1}(t)\cos(2\pi f_c t + b_k\pi) + n_1(t), \quad (10)$$

where $n_1(t)$ is the receiver noise at the first relay node. The relay node first normalizes the received signal to ensure the unity of average signal power as

$$e_1(t) = X_{0,1}\cos(2\pi f_c t + b_k\pi) + \frac{n_1(t)}{\Re\bar{g}\frac{P_s}{2}a_{0,1}}. \quad (11)$$

The normalized electrical signal $e_1(t)$ is then used to modulate the intensity of the optical beam with a peak power P_s and re-transmitted to the next relay node (or the destination). Hence, the transmitted optical signal for the next transmission can be written as

$$s_1(t) = \frac{P_s}{2}\left[1 + X_{0,1}\cos(2\pi f_c t + b_k\pi) + \frac{n_1(t)}{\Re\bar{g}\frac{P_s}{2}a_{0,1}}\right]. \quad (12)$$

Repeating the above manipulations, the electrical current out of the APD at the i-th relay node can be expressed as

$$r_i(t) = \Re\bar{g}\frac{P_s}{2}a_{i-1,i}\prod_{j=1}^{i}X_{j-1,j}\cos(2\pi f_c t + b_k\pi) + \sum_{j=1}^{i-1}\frac{n_j(t)a_{i-1,i}\prod_{k=j+1}^{i}X_{k-1,k}}{a_{j-1,j}} + n_i(t). \quad (13)$$

For $i = 1$, the above equation simplifies to Eq. (10).

2.3.2 Parallel Configuration

In this configuration, the source transmits signal to all relay nodes directly and simultaneously. Therefore, the output electrical signal of the APD at the $i-$th relay node (i =

1, 2, ..., N) is given by

$$r_i(t) = \Re\bar{g}\frac{P_s}{2}a_{0,i}X_{0,i}(t)\cos(2\pi f_c t + b_k\pi) + n_i(t). \quad (14)$$

Similar to the serial relaying scheme, each relay node normalizes its received signal, then modulates the normalized signal by an optical power P_s and retransmits it to the destination. Thus, the received signal at the destination can be obtained by adding individual transmitted signals from N relay nodes as

$$r_{N+1}(t) = \Re\bar{g}\frac{P_s}{2}\cos(2\pi f_c t + b_k\pi)\sum_{i=1}^{N} a_{i,N+1}X_{0,i}X_{i,N+1} + \sum_{i=1}^{N}\frac{a_{N+1}X_{i,N+1}n_i(t)}{a_{0,i}} + n_{N+1}(t). \quad (15)$$

3. Performance Analysis

3.1 Outage Probability

At a given transmission rate R, the outage probability of a communication channel is defined by

$$P_{out} = \Pr(C(\gamma) < R), \quad (16)$$

where $C(\gamma)$ is the instantaneous capacity of the channel, and γ is the instantaneous signal-to-noise ratio (SNR). As C increases monotonically with respect to γ, the outage probability can be represented by another formula as

$$P_{out} = \Pr(\gamma < \gamma_{th}) = 1 - \Pr\left(\frac{1}{\gamma} < \frac{1}{\gamma_{th}}\right), \quad (17)$$

where $\gamma_{th} = C^{-1}(R)$ is the threshold SNR that is required to support the data rate R. In other words, when the SNR γ exceeds γ_{th}, there will be no outage and the signal can be decoded with an arbitrarily low error probability at the receiver. In practice, γ_{th} is set based on modulation scheme and targeted spectral efficiency. For the sake of simulation runtime, we use $\gamma_{th} = 8$ dB, which corresponds to the spectral efficiency of 1 bit/s/Hz and binary signalling [22]. In the AF relaying, because all relay nodes just scale the received signal without any decoding, the outage probability of the system is also defined as the probability that the end-to-end instantaneous SNR (also denoted as γ) falls bellow γ_{th}.

In this section, we use the following definitions $A = (\Re\bar{g}P_t)^2$, $B = \frac{4k_BT}{R_L}F_n\Delta f$, $C = 2q\bar{g}^2F_A\Re\left(\frac{P_t}{4}\right)\Delta f$, $Z_1 = \frac{16N_r^2B}{A}$, and $Z_2 = \frac{16N_rC}{A}$.

3.1.1 Serial Configuration

From Eq. (13), the inverse end-to-end SNR can be obtained by

$$\frac{1}{\gamma} = \sum_{i=1}^{N+1}\frac{Z_1}{a_{i-1,i}^2\prod_{j=1}^{i}X_{j-1,j}^2} + \sum_{i=1}^{N+1}\frac{Z_2}{a_{i-1,i}\prod_{j=1}^{i}X_{j-1,j}}. \quad (21)$$

For simplicity, we define $\tau_i = \frac{Z_1}{a_{i-1,i}^2\prod_{j=1}^{i}X_{j-1,j}^2}$, $\upsilon_i = \frac{Z_2}{a_{i-1,i}\prod_{j=1}^{i}X_{j-1,j}}$. Obviously, τ_i and υ_i are correlated log-normal random variables. It is known that the sum of τ_i's and υ_i's can be approximated as a single log-normal random variable by several methods [23]–[27]. In this study, we employ the well-known Fenton-Wilkinson method [23], [24], in which $\frac{1}{\gamma}$ is approximated by a log-normal random variable z_1 whose parameters are μ_{z_1} and σ_{z_1}

$$z_1 \approx \frac{1}{\gamma}. \quad (22)$$

The end-to-end outage probability of the serial relaying system therefore can be obtained as

$$P_{out} \approx 1 - \Pr\left(z_1 < \frac{1}{\gamma_{th}}\right) = \frac{1}{2}\mathrm{erfc}\left(\frac{\ln(\frac{1}{\gamma_{th}}) - \mu_{z_1}}{\sqrt{2\sigma_{z_1}^2}}\right), \quad (23)$$

where $\mathrm{erfc}(x) = (2/\sqrt{\pi})\int_x^\infty e^{-t^2}\mathrm{d}t$ is the complementary error function.

The derivations of μ_{z_1} and σ_{z_1} can be found in the Appendix A. It should be noted that there are several other approximation methods [25]–[27] that generally provide a better approximation than the Fenton-Wilkinson method. Nonetheless, the accuracy of those methods comes at the expense of high computational complexity, especially for the case of sum of correlated random variables as in this study.

3.1.2 Parallel Configuration

From Eq. (15), the inverse end-to-end SNR of the parallel relaying scheme can be derived as in Eq. (18) at the top of the next page. Each summation term in the numerator and denominator can be approximated by a single log-normal random variable as represented in Eqs. (19) and (20), respectively. Eq. (18) therefore can be rewritten as

$$\frac{1}{\gamma} \approx \frac{e^{\varphi_1} + Z_1}{e^{2\varphi_2}} = e^{\varphi_1 - 2\varphi_2} + e^{\ln(Z_1) - 2\varphi_2}. \quad (24)$$

Similar to the case of serial configuration, $\frac{1}{\gamma}$ can also be approximated by a log-normal random variable z_2 whose parameters are μ_{z_2} and σ_{z_2}. For derivations of μ_{z_1} and σ_{z_2}, please refer to the Appendix B. We are now able to derive the the end-to-end outage probability of the parallel laying scheme as

$$P_{out} \approx 1 - \Pr\left(z_2 < \frac{1}{\gamma_{th}}\right) = \frac{1}{2}\mathrm{erfc}\left(\frac{\ln(\frac{1}{\gamma_{th}}) - \mu_{z_2}}{\sqrt{2\sigma_{z_2}^2}}\right). \quad (25)$$

3.2 Bit-Error Rate

In FSO systems, as the temporal correlation time of the

$$\frac{1}{\gamma} = \frac{Z_1\left(\sum_{i=1}^{N}\frac{a_{i,N+1}^2}{a_{0,i}^2}X_{i,N+1}^2+1\right)+Z_2\left(\sum_{i=1}^{N}\frac{a_{i,N+1}^2}{a_{0,i}}X_{i,N+1}^2X_{0,i}+\sum_{i=1}^{N}a_{i,N+1}X_{0,i}X_{i,N+1}\right)}{\left(\sum_{i=1}^{N}a_{i,N+1}X_{0,i}X_{i,N+1}\right)^2}. \tag{18}$$

$$e^{\varphi_1} \approx Z_1\left(\sum_{i=1}^{N}\frac{a_{i,N+1}^2}{a_{0,i}^2}X_{i,N+1}^2\right)+Z_2\left(\sum_{i=1}^{N}\frac{a_{i,N+1}^2}{a_{0,i}}X_{i,N+1}^2X_{0,i}+\sum_{i=1}^{N}a_{i,N+1}X_{0,i}X_{i,N+1}\right). \tag{19}$$

$$e^{\varphi_2} \approx \sum_{i=1}^{N}a_{i,N+1}X_{0,i}X_{i,N+1}. \tag{20}$$

atmospheric scintillation process is in the order of several milliseconds, which is much longer than a bit duration, the average BER over the turbulence channel can be expressed as

$$P_e = \int_0^\infty P_{e-i}(\gamma)f_\gamma(\gamma)\mathrm{d}\gamma, \tag{26}$$

where γ is the instantaneous SNR at the destination, which can be obtained from Eqs. (21) and (18) for serial and parallel configurations, respectively. $f_\gamma(\gamma)$ is the pdf of γ and $P_{e-i}(\gamma)$ denotes the conditional BER given the received instantaneous SNR γ. For the case of BPSK modulation, $P_{e-i}(\gamma)$ is given by

$$P_{e-i}(\gamma) = Q(\sqrt{\gamma}), \tag{27}$$

where $Q(x) = \frac{1}{\sqrt{2\pi}}\int_x^\infty \exp(-\frac{u^2}{2})\mathrm{d}u$ is the Gaussian-Q function [3].

Plugging (27) into (26), the average end-to-end BER can be rewritten as

$$P_e = \int_0^\infty Q(\sqrt{\gamma})f_\gamma(\gamma)\mathrm{d}\gamma. \tag{28}$$

3.2.1 Serial Configuration

Since the inverse end-to-end SNR $\frac{1}{\gamma}$ has been approximated by the single log-normal random variable z_1 as presented in the previous section, the SNR γ can be approximated as a log-normal random variable z_1' whose logarithm mean is $-\mu_{z_1}$ and logarithm variance is $\sigma_{z_1}^2$. The average BER of serial relaying therefore is given following Eq. (28) as

$$P_e \approx \int_0^\infty Q\left(\sqrt{2z_1'}\right) \times \frac{1}{\sqrt{2\pi}\sigma_{z_1}z_1'}\exp\left[-\frac{(\ln z_1'+\mu_{z_1})^2}{2\sigma_{z_1}^2}\right]\mathrm{d}z_1'. \tag{29}$$

Making the change of variable $y = (\ln z_1' + \mu_{z_1})/\sqrt{2}\sigma_{z_1}$, we have

$$P_e \approx \frac{1}{\sqrt{\pi}}\int_{-\infty}^\infty Q\left(\sqrt{\exp\left[\sqrt{2}y\sigma_{z_1}-\mu_{z_1}\right]}\right) \times \exp(-y^2)\mathrm{d}y. \tag{30}$$

According to the following approximation

$$\int_{-\infty}^\infty f(x)\exp(-x^2) \approx \frac{1}{\sqrt{\pi}}\sum_{i=-N,i\neq 0}^{N} w_i f(x_i), \tag{31}$$

where w_i and x_i are the weighting vectors and the zeros of the Hermite polynomial, respectively [28], P_e can be expressed in a tractable form as

$$P_e \approx \frac{1}{\pi}\sum_{i=-N,i\neq 0}^{N} w_i Q\left(\sqrt{\exp\left[\sqrt{2}y_i\sigma_{z_1}-\mu_{z_1}\right]}\right). \tag{32}$$

3.2.2 Parallel Configuration

Similar to the case of serial relaying, the average BER of parallel relaying can be obtained by

$$P_e \approx \frac{1}{\pi}\sum_{i=-N,i\neq 0}^{N} w_i Q\left(\sqrt{\exp\left[\sqrt{2}y_i\sigma_{z_2}-\mu_{z_2}\right]}\right), \tag{33}$$

where μ_{z_2}, σ_{z_2} are respectively the logarithm mean and logarithm standard deviation of the log-normal random variable z_2 mentioned in Sect. 3.1.2.

4. Numerical Results & Discussions

This section presents representative numerical results and discussions regarding the outage probability and the BER analytically derived in Sect. 3. In addition, Monte-Carlo simulations are used to validate the analytical results. The distance from the source to the destination $L = 2$ km is set. For the serial configuration, it is assumed that the distances between any two consecutive nodes are equal. In the parallel configuration, the relay nodes are placed at the halfway point (i.e., the middle point between the source and the destination). For mathematical convenience, it is assumed that the differences in distances from the source to the relay nodes are negligible and they all can be assumed to be equal to $L/2$[†]. In the numerical results, we use the

[†]This assumption is practically acceptable and widely used in studies of parallel systems as the distance between the source/destination to relay node is in the order of thousand meters [5], [7], [14].

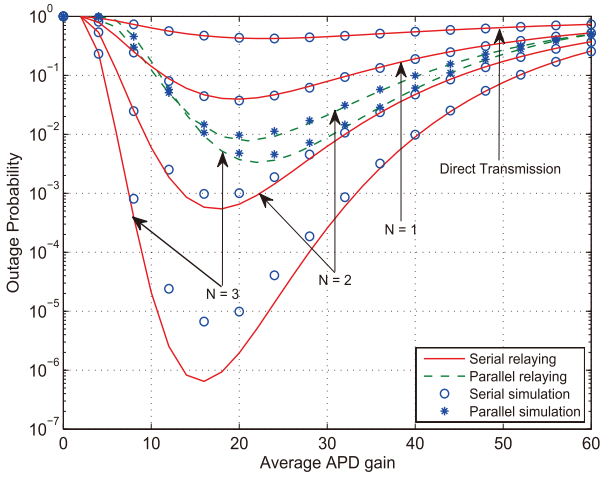

Fig. 4 Outage probability versus average APD gain for both serial and parallel configurations.

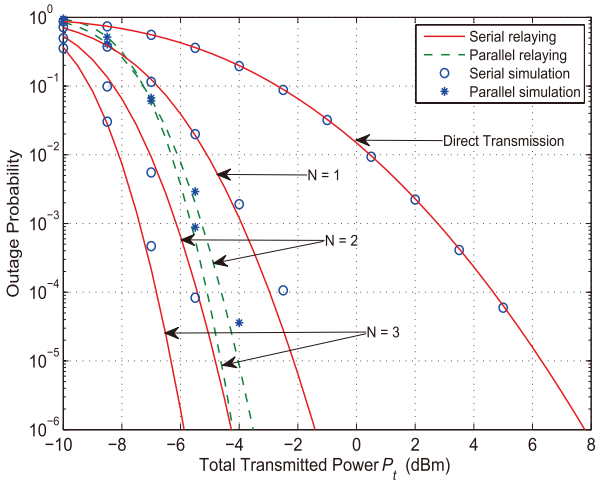

Fig. 5 Outage probability versus total transmitted power P_t for both serial and parallel configurations.

turbulence strength $C_n^2 = 8 \times 10^{-15}$ m$^{-2/3}$ and the atmospheric extinction coefficient $\beta_\nu = 0.1$ dB/km. Unless otherwise noted, the system parameters are chosen as follows: optical wavelength $\lambda = 1550$ nm, the APD load resistance $R_L = 1000\ \Omega$, the amplifier noise figure $F_n = 2$, the system bit rate $R_b = 2$ Gbps, the ionization factor $k_A = 0.7$, and the aperture diameter $D = 0.03$ m.

4.1 Outage Probability

First, Fig. 4 shows the outage probability versus the average APD gain for both serial and parallel configurations when the total transmitted power $P_t = -6$ dBm is set. Similar to the single hop systems [3], there exists an optimal APD gain value where the lowest outage probability can be achieved. Thus, the outage performance of the APD-based AF relaying systems is greatly benefited from a proper selection of the APD gain value. It is seen that when the number of relay nodes is changed, the optimal gain values are almost the same in the parallel configuration. However, the optimal gain value reduces as the number of relay nodes increases in the serial configuration. Monte-Carlo simulations reveal a fair accuracy of the Fenton-Wilkinson method. It is also seen that the accuracy is not good around the optimal gain value due to the limit of the Fenton-Wilkinson method in the case of the high values of standard deviations of the summands due to the approximation via the inverse SNR in the previous section. The approximation results are nevertheless acceptable since the optimum APD gain values obtained from the approximations and the simulations are almost the same.

Next, Fig. 5 shows the outage probability of serial and parallel relaying schemes versus the total transmitted power with different numbers of relay nodes. The average APD gain $\overline{g} = 20$, which is close to the optimal gain values as shown in Fig. 4, is set. We also use the Monte-Carlo simulation to validate the analytical results. As expected, we can observe that an increase in the number of relay nodes results in a better performance in both cases of relay configuration.

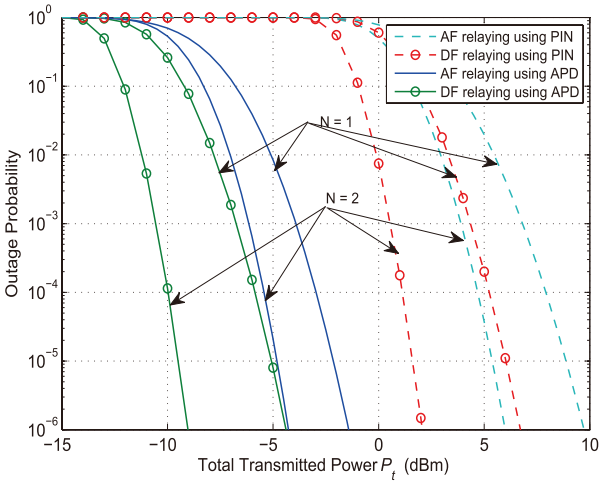

Fig. 6 Outage probability of APD-based AF versus DF systems using PIN and APD receivers (serial configuration).

In particular, at the outage probability of 10^{-6}, the power gains compared with direct transmission, when the number of relay nodes $N = 1$, 2, and 3, are 9 dB, 12 dB, 13.7 dB for serial relaying and 9.5 dB, 11.2 dB, 12 dB for parallel relaying, respectively. Furthermore, we can verify a good agreement between the analytical and simulation results, which confirms the validity of the approximation analysis.

In Fig. 6, we illustrate the superiority of the use of APD receiver in comparison with PIN-based relaying systems. The APD gain $\overline{g} = 20$ is also used. The main difference of PIN from APD is that it does not provide internal current gain as APD does [29]. It leads to an obvious consequence that the APD-based systems can achieve a better performance than that of a similar systems using PIN receiver. Nevertheless, the key finding is that the proposed APD-based AF system is still able to offer a better performance than that of PIN-based DF systems. This is the main advantage of the proposed system as it is essentially simpler than the DF ones.

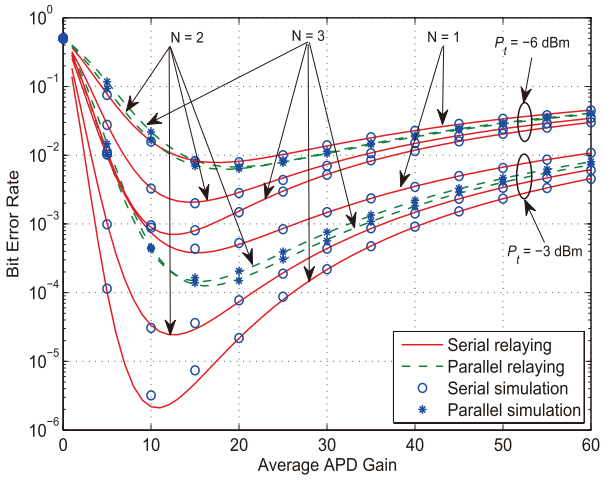

Fig. 7 BER versus average APD gain for both serial and parallel configurations.

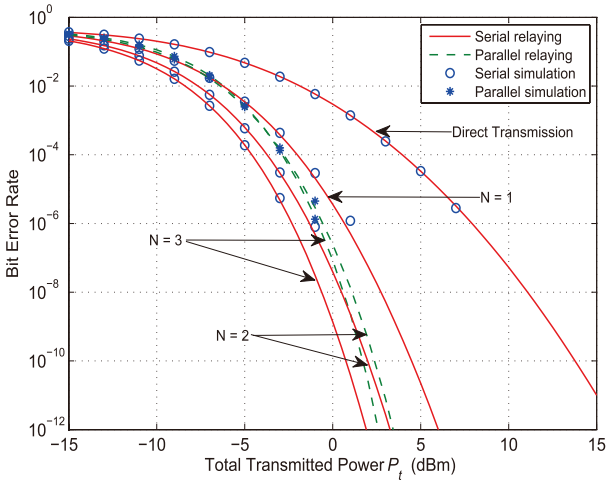

Fig. 8 BER vs. total transmitted power P_t for both serial and parallel configurations.

Quantitatively, using APD receivers for AF systems results in about 6 dB or 4 dB gains in comparison with the case of PIN-based DF approach when there are 1 or 2 relay nodes, respectively.

4.2 Bit-Error Rate

Now, we investigate the BER performance of the proposed system. First, Fig. 7 shows the BER of serial and parallel relaying schemes versus the average APD gain for different the total transmitted power $P_t = -3$ dBm and -6 dBm, respectively. Again, we also see that, in both relay configurations, there always exists an optimal APD gain values where the lowest BER performance can be achieved. It is observed that the optimal gain values for the same number of relay nodes and relaying scheme in both cases of the total transmitted power are almost unchanged. Nevertheless, it is noteworthy to mention that the optimal gain values for the BER and outage probability are not always the same due to the fact that the outage probability is additionally dependent on the value of threshold SNR. A proper selection of APD gain taking into account the number of relay nodes as well as the expected performance is therefore highly recommended.

Next, Fig. 8 depicts the BER as a function of the total transmitted power P_t for serial and parallel configurations. The APD gain is chosen to be 15. Similar to the outage performance, we can observe that an increase in the number of relay nodes results in a better performance in both relay configurations, especially in the serial one. This is because the serial systems could significantly remedy the distance-dependent atmospheric turbulence by using additional relay nodes. Again, the well-matched Monte-Carlo simulation results confirm the validity of the theoretical analysis.

Finally, Fig. 9 shows the BER performance comparison between two systems: DF and AF relaying for different type of receivers: PIN and APD with the APD gain $\bar{g}$ is set to be 15. As expected, APD-based relaying systems outperform the PIN-based ones in the case of the same relaying strategy.

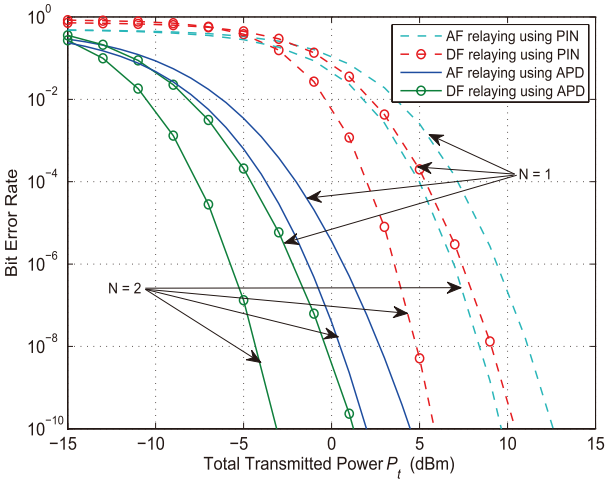

Fig. 9 BER of APD-based AF versus DF systems using PIN and APD receivers (serial configuration).

We could also confirm the main advantage of the proposed APD-based AF system is that it could offer a better performance than that of the DF using PIN receiver. At the BER of 10^{-10}, the power gains of the proposed system compared with the DF relaying using PIN system are 6 dB, 4 dB when $N = 1, 2$, respectively.

5. Conclusions

We proposed and theoretically analyzed the performance of APD-based AF relaying FSO systems using SC-BPSK signaling over atmospheric turbulence channels. Closed-form expressions for the outage probability and the BER were analytically derived for both serial and parallel configurations. Monte-Carlo simulations were used to confirm the theoretical analysis, and a good agreement between simulation and theoretical results was confirmed. As expected, the performance of FSO systems could be improved significantly with

the help of relay nodes. We also compared the outage and the BER performance of the proposed AF system with that of the DF system using PIN receiver. Numerical results confirmed that the proposed system offered an essential gain with a less complex structure. Furthermore, the selection of APD gain could greatly affect the performance of the system and there always exists an optimal APD gain value for achieving the best performance.

References

[1] H. Willebrand and B.S. Ghuman, Free-Space Optics: Enabling Optical Connectivity in Today's Networks, Sams Publishing, 2001.
[2] S. Karp, Optical channels: fibers, clouds, water and the atmosphere, Plenum Press, 1988.
[3] D.A. Luong, C.T. Truong, and A.T. Pham, "Effect of APD and thermal noises on the performance of SC-BPSK/FSO systems over turbulence channels," 2012 18th Asia-Pacific Conference on Communications (APCC), pp.344–349, 2012.
[4] T.A. Tsiftsis, H.G. Sandalidis, G.K. Karagiannidis, and N.C. Sagias, "Multihop free-space optical communications over strong turbulence channels," Proc. 2006 IEEE International Conference on Communications, vol.6, pp.2755–2759, June 2006.
[5] N.D. Chatzidiamantis, D.S. Michalopoulos, E.E. Kriezis, G.K. Karagiannidis, and R. Schober, "Relay selection protocols for relay-assisted free-space optical systems," J. Opt. Commun. Netw., vol.5, no.1, pp.92–103, Jan. 2013.
[6] T.V. Pham and A.T. Pham, "Performance analysis of amplify-decode-and-forward multihop BPSK/FSO systems using APD receivers over atmospheric turbulence channels," IET Commun., vol.8, no.9, pp.1518–1526, June 2014.
[7] M. Safari and M. Uysal, "Relay-assisted free-space optical communication," IEEE Trans. Wireless Commun., vol.7, no.12, pp.5441–5449, Dec. 2008.
[8] L. Yang, X. Gao, and M.-S. Alouini, "Performance analysis of relay-assisted all-optical FSO networks over strong atmospheric turbulence channels with pointing errors," J. Lightwave Technol., vol.32, no.23, pp.4613–4620, Dec. 2014.
[9] C. Abou-Rjeily, "Performance analysis of selective relaying in cooperative free-space optical systems," J. Lightwave Technol., vol.31, no.18, pp.2965–2973, Sept. 2013.
[10] K.P. Peppas, A.N. Stassinakis, H.E. Nistazakis, and G.S. Tombras, "Capacity analysis of dual amplify-and-forward relayed free-space optical communication systems over turbulence channels with pointing errors," J. Opt. Commun. Netw., vol.5, no.9, pp.1032–1042, Sept. 2013.
[11] M. Aggarwal, P. Garg, and P. Puri, "Dual-hop optical wireless relaying over turbulence channels with pointing error impairments," J. Lightwave Technol., vol.32, no.9, pp.1821–1828, May 2014.
[12] S. Kazemlou, S. Hranilovic, and S. Kumar, "All-optical multihop free-space optical communication systems," J. Lightwave Technol., vol.29, no.18, pp.2663–2669, Sept. 2011.
[13] M. Karimi and M. Nasiri-Kenari, "Free space optical communications via optical amplify-and-forward relaying," J. Lightwave Technol., vol.29, no.2, pp.242–248, Jan. 2011.
[14] J.Y. Wang, J.B. Wang, M. Chen, and X. Song, "Performance analysis for free-space optical communications using parallel all-optical relays over composite channels," IET Commun., vol.8, no.9, pp.1437–1446, June 2014.
[15] E. Bayaki, D.S. Michalopoulos, and R. Schober, "EDFA-based all-optical relaying in free-space optical systems," IEEE Trans. Commun., vol.60, no.12, pp.3797–3807, Dec. 2012.
[16] M.A. Kashani, M.M. Rad, M. Safari, and M. Uysal, "All-optical amplify-and-forward relaying system for atmospheric channels," IEEE Commun. Lett., vol.16, no.10, pp.1684–1687, Oct. 2012.
[17] P.V. Trinh, A.T. Pham, H.T.T. Pham, and N.T. Dang, "BER analysis of all-optical AF dual-hop FSO systems over Gamma-Gamma channels," Proc. 2013 IEEE 4th International Conference on Photonics (ICP), pp.175–177, Oct. 2013.
[18] X. Zhu and J.M. Kahn, "Free-space optical communication through atmospheric turbulence channels," IEEE Trans. Commun., vol.50, no.8, pp.1293–1300, Aug. 2002.
[19] S.G. Wilson, M. Brandt-Pearce, Q. Cao, and M. Baedke, "Optical repetition MIMO transmission with multipulse PPM," IEEE J. Sel. Areas Commun., vol.23, no.9, pp.1901–1910, Sept. 2005.
[20] W. Huang, J. Takayanagi, T. Sakanaka, and M. Nakagawa, "Atmospheric optical communication system using subcarrier PSK modulation," IEICE Trans. Commun., vol.E76-B, no.9, pp.1169–1177, Sept. 1993.
[21] J.W. Goodman, Statistical optics, John Wiley & Sons, 1985.
[22] J.G. Proakis, Digital Communications, 4th ed., McGraw-Hill, 2001.
[23] L. Fenton, "The sum of log-normal probability distributions in scatter transmission systems," IRE Trans. Commun., Syst., vol.8, no.1, pp.57–67, March 1960.
[24] A.A. Abu-Dayya and N.C. Beaulieu, "Outage probabilities in the presence of correlated lognormal interferers," IEEE Trans. Veh. Technol., vol.43, no.1, pp.164–173, Feb. 1994.
[25] S.C. Schwartz and Y.S. Yeh, "On the distribution function and moments of power sums with log-normal components," Bell Syst. Tech. J., vol.61, no.7, pp.1441–1462, Sept. 1982.
[26] N.B. Mehta, J. Wu, A.F. Molisch, and J. Zhang, "Approximating a sum of random variables with a lognormal," IEEE Trans. Wireless Commun., vol.6, no.7, pp.2690–2699, July 2007.
[27] C.L.J. Lam and T. Le-Ngoc, "Log-shifted gamma approximation to lognormal sum distributions," IEEE Trans. Veh. Technol., vol.56, no.4, pp.2121–2129, July 2007.
[28] M. Abramowitz and I.A. Stegun, Handbook of mathematical functions, with formulas, graphs, and mathematical tables, 9th ed., National Bureau of Standards, 1970.
[29] G.P. Agrawal, Fiber-optic communication systems, 3rd ed., John Wiley & Sons, 2002.

Appendix A: Derivations of μ_{z_1} and σ_{z_1}

For two normal random variables x_i and y_j, we denote $M_x(i) = e^{\mu_{x_i}+\sigma^2_{x_i}/2}$, $L_x(i) = e^{2\mu_{x_i}+2\sigma^2_{x_i}}$, $K_{x,y}(i,j) = 2e^{\mu_{x_i}+\mu_{y_j}+\frac{1}{2}(\sigma^2_{x_i}+\sigma^2_{y_j}+2\Lambda_{x,y}(i,j))}$, where $\mu_{x_i}, \sigma^2_{x_i}, \Lambda_{x,y}(i,j)$ represent the mean, the variance of x_i and the covariance between (x_i, y_j), respectively.

Since τ_i and υ_i are log-normal random variables, they can be expressed as $\tau_i = \exp(\omega_i)$, $\upsilon_i = \exp(\psi_i)$. Here, ω_i and ψ_i are normally distributed with their means and variances are given by

$$\mu_{\omega_i} = \ln\left(\frac{Z_1}{a^2_{i-1,i}}\right) + 2\sum_{j=1}^{i}\sigma^2_s(\ell_{j-1,j}), \tag{A·1}$$

$$\sigma^2_{\omega_i} = 4\sum_{j=1}^{i}\sigma^2_s(\ell_{j-1,j}), \tag{A·2}$$

and,

$$\mu_{\psi_i} = \ln\left(\frac{Z_2}{a_{i-1,i}}\right) + \sum_{j=1}^{i}\sigma^2_s(\ell_{j-1,j}), \tag{A·3}$$

$$\Delta = Z_1 \sum_{i=1}^{N} \left(e^{\sigma_s^2(\ell_{i,N+1})} - e^{-\sigma_s^2(\ell_{i,N+1})}\right) + Z_2 \sum_{i=1}^{N} \left(e^{\frac{3}{2}\sigma_s^2(\ell_{i,N+1})} - e^{-\sigma_s^2(\ell_{0,i}) - \frac{1}{2}\sigma_s^2(\ell_{i,N+1})}\right) + Z_2 \sum_{i=1}^{N} \left(1 - e^{-\sigma_s^2(\ell_{0,i}) - \sigma_s^2(\ell_{i,N+1})}\right) \quad (A\cdot 22)$$

$$\sigma_{\psi_i}^2 = \sum_{j=1}^{i} \sigma_s^2(\ell_{j-1,j}). \quad (A\cdot 4)$$

The covariances between (ω_i, ω_j), (ψ_i, ψ_j), (ω_i, ψ_j) are given by $\Lambda_{\omega,\omega}(i,j) = \sigma_{\omega_k}^2(k = \min(i,j))$, $\Lambda_{\psi,\psi}(i,j) = \sigma_{\psi_k}^2(k = \min(i,j))$ and $\Lambda_{\omega,\psi}(i,j) = 2\sum_{k=1}^{\min(i,j)} \sigma_s^2(\ell_{k-1,k})$, respectively.

Using the Fenton-Wilkinson method, logarithm mean μ_{z_1} and logarithm variance $\sigma_{z_1}^2$ of z_1 can be derived as $\mu_{z_1} = 2\ln(u_1) - 1/2\ln(u_2)$ and $\sigma_{z_1}^2 = \ln(u_2) - 2\ln(u_1)$, where u_1, u_2 are obtained by

$$u_1 = \sum_{i=1}^{N+1} \left(M_\omega(i) + M_\psi(i)\right), \quad (A\cdot 5)$$

$$u_2 = \sum_{i=1}^{N+1} \left(L_\omega(i) + L_\psi(i)\right) + \sum_{i=1}^{N} \sum_{j=i+1}^{N+1} \left(K_{\omega,\omega}(i,j) + K_{\psi,\psi}(i,j)\right) + \sum_{i=1}^{N+1} \sum_{j=1}^{N+1} K_{\omega,\psi}(i,j). \quad (A\cdot 6)$$

Appendix B: Derivations of μ_{z_2} and σ_{z_2}

In this part, we use the following definitions $e^{\epsilon_i} = Z_1 \frac{a_{i,N+1}^2}{a_{0,i}^2} X_{i,N+1}^2$, $e^{\nu_i} = Z_2 \frac{a_{i,N+1}^2}{a_{0,i}} X_{0,i} X_{i,N+1}^2$ and $e^{\kappa_i} = Z_2 a_{i,N+1} X_{0,i} X_{i,N+1}$. Here, ϵ_i, ν_i and κ_i are normal random variables with their means and variances given by

$$\mu_{\epsilon_i} = \ln\left(Z_1 \frac{a_{i,N+1}^2}{a_{0,i}^2}\right) - 2\sigma_s^2(\ell_{i,N+1}), \quad (A\cdot 7)$$

$$\sigma_{\epsilon_i}^2 = 4\sigma_s^2(\ell_{i,N+1}); \quad (A\cdot 8)$$

$$\mu_{\nu_i} = \ln\left(Z_2 \frac{a_{i,N+1}^2}{a_{0,i}}\right) - \sigma_s^2(\ell_{0,i}) - 2\sigma_s^2(\ell_{i,N+1}), \quad (A\cdot 9)$$

$$\sigma_{\nu_i}^2 = \sigma_s^2(\ell_{0,i}) + 4\sigma_s^2(\ell_{i,N+1}); \quad (A\cdot 10)$$

$$\mu_{\kappa_i} = \ln\left(Z_2 a_{i,N+1}\right) - \sigma_s^2(\ell_{0,i}) - \sigma_s^2(\ell_{i,N+1}), \quad (A\cdot 11)$$

$$\sigma_{\kappa_i}^2 = \sigma_s^2(\ell_{0,i}) + \sigma_s^2(\ell_{i,N+1}). \quad (A\cdot 12)$$

Obviously, the covariances between (ϵ_i, ϵ_j), (ν_i, ν_j), (κ_i, κ_j) are 0. On the other hand, the covariances between (ϵ_i, ν_j), (ϵ_i, κ_j), (ν_i, κ_j) can be obtained as

$$\Lambda_{\epsilon,\nu}(i,j) = \begin{cases} 4\sigma_s^2(\ell_{i,N+1}) & i = j \\ 0 & i \neq j \end{cases} \quad (A\cdot 13)$$

$$\Lambda_{\epsilon,\kappa}(i,j) = \begin{cases} 2\sigma_s^2(\ell_{i,N+1}) & i = j \\ 0 & i \neq j \end{cases} \quad (A\cdot 14)$$

$$\Lambda_{\nu,\kappa}(i,j) = \begin{cases} \sigma_s^2(\ell_{0,i}) + 2\sigma_s^2(\ell_{i,N+1}) & i = j \\ 0 & i \neq j \end{cases} \quad (A\cdot 15)$$

Using the Fenton-Wilkinson method, the mean and variance of φ_1 can be derived as $\mu_{\varphi_1} = 2\ln(v_1) - 1/2\ln(v_2)$ and $\sigma_{\varphi_1}^2 = \ln(v_2) - 2\ln(v_1)$, where v_1, v_2 are given by

$$v_1 = \sum_{i=1}^{N} \left(M_\epsilon(i) + M_\nu(i) + M_\kappa(i)\right), \quad (A\cdot 16)$$

$$v_2 = \sum_{i=1}^{N} \left(L_\epsilon(i) + L_\nu(i) + L_\kappa(i)\right) + \sum_{i=1}^{N-1} \sum_{j=i+1}^{N} \left(K_{\epsilon,\epsilon}(i,j) + K_{\nu,\nu}(i,j) + K_{\kappa,\kappa}(i,j)\right) + \sum_{i=1}^{N} \sum_{j=1}^{N} \left[K_{\epsilon,\nu}(i,j) + K_{\epsilon,\kappa}(i,j) + K_{\nu,\kappa}(i,j)\right]. \quad (A\cdot 17)$$

Similarly, following that approximation method, the mean and variance of φ_2 can be written as

$$\mu_{\varphi_2} = \ln\left(\sum_{i=1}^{N} e^{\rho_i}\right) - \sigma_{\varphi_2}^2/2, \quad (A\cdot 18)$$

$$\sigma_{\varphi_2}^2 = \ln\left(1 + \frac{\sum_{i=1}^{N} e^{2\rho_i}\left(e^{\sigma_s^2(\ell_{0,i}) + \sigma_s^2(\ell_{i,N+1})} - 1\right)}{\left(\sum_{i=1}^{N} e^{\rho_i}\right)^2}\right), \quad (A\cdot 19)$$

in which ρ_i is defined by

$$\rho_i = \ln(a_{i,N+1}) - \frac{1}{2}\left[\sigma_s^2(\ell_{0,i}) + \sigma_s^2(\ell_{i,N+1})\right]. \quad (A\cdot 20)$$

On the other hand, the covariance between $(\varphi_1 - 2\varphi_2, \ln(Z_1) - 2\varphi_2)$ can be obtained as $\Lambda = 4\sigma_{\varphi_2}^2 - 2\Lambda_{\varphi_1,\varphi_2}$. Here, $\Lambda_{\varphi_1,\varphi_2}$ denotes the covariance between (φ_1, φ_2) and can be expressed by

$$\Lambda_{\varphi_1,\varphi_2} = \ln\left(1 + \frac{\Delta}{e^{\mu_{\varphi_1} + \mu_{\varphi_2} + (\sigma_{\varphi_2}^2 + \sigma_{\varphi_2}^2)/2}}\right), \quad (A\cdot 21)$$

where Δ is the covariance between $(e^{\varphi_1}, e^{\varphi_2})$ and is given by Eq. (A·22) at the top of this page.

Thus, $\frac{1}{\gamma}$ can be approximated as a single log-normal random variable z_2 whose logarithm mean $\mu_{z_2} = 2\ln(t_1) - 1/2\ln(t_2)$ and logarithm variance $\sigma_{z_2}^2 = \ln(t_2) - 2\ln(t_1)$, where t_1 and t_2 are derived by

$$t_1 = e^{\mu_{\varphi_1} - 2\mu_{\varphi_2} + \frac{1}{2}(\sigma^2_{\varphi_1} + 4\sigma^2_{\varphi_2} - 4\Lambda_{\varphi_1,\varphi_2})} + e^{\ln(Z_1) - 2\mu_{\varphi_2} + 2\sigma^2_{\varphi_2}}, \quad \text{(A·23)}$$

$$t_2 = e^{2\mu_{\varphi_1} - 4\mu_{\varphi_2} + 2(\sigma^2_{\varphi_1} + 4\sigma^2_{\varphi_2} - 4\Lambda_{\varphi_1,\varphi_2})} + e^{2\ln(Z_1) - 4\mu_{\varphi_2} + 8\sigma^2_{\varphi_2}} + 2e^{\mu_{\varphi_1} + \ln(Z_1) - 4\mu_{\varphi_2} + \frac{1}{2}(\sigma^2_{\varphi_1} + 8\sigma^2_{\varphi_2} - 4\Lambda_{\varphi_1,\varphi_2} + 2\Lambda)}. \quad \text{(A·24)}$$

Thanh V. Pham received the B.E. degree in Computer Network Systems from the University of Aizu, Japan in 2014. He is currently studying toward a M.E degree also at the University of Aizu. His study in Japan is funded by Japanese government scholarship (MonbuKagaku-sho). His research interests are in the area of free-space optics (FSO), relay networks and Visible Light Communications (VLC). Thanh, as the undergraduate student, is awarded the "Encouragement Prize" by IEEE Sendai Section for his paper presented at the 2013 Tohoku-Section Joint Convention of Institutes of Electrical and Information Engineers, Japan. Thanh is a student member of IEEE.

Anh T. Pham received the B.E. and M.E. degrees, both in Electronics Engineering from the Hanoi University of Technology, Vietnam in 1997 and 2000, respectively, and the Ph.D. degree in Information and Mathematical Sciences from Saitama University, Japan in 2005. From 1998 to 2002, he was with the NTT Corp. in Vietnam. Since April 2005, he has been on the faculty at the University of Aizu, where he is currently Professor and Head of Computer Communications Laboratory with the Division of Computer Engineering. Professor Pham's research interests are in the broad areas of communication theory and networking with a particular emphasis on modeling, design and performance evaluation of wired/wireless communication systems and networks. He has authored/co-authored more than 130 peer-reviewed papers, including 40+ journal articles, on these topics. Professor Pham is a senior member of IEEE. He is also member of IEICE and OSA.